NANO LETTERS

2005
Vol. 5, No. 8
1545−1549

Nanostructuring Titania by Embossing with Polymer Molds Made from Anodic Alumina Templates

Chiatzun Goh, Kevin M. Coakley, and Michael D. McGehee*

Department of Materials Science & Engineering, Stanford University, Stanford, California 94305

Received April 15, 2005; Revised Manuscript Received June 30, 2005

ABSTRACT

We demonstrate a method for embossing titania sol–gel precursor with poly(methyl methacrylate) (PMMA) molds to make thin films of titania that have dense arrays of 35–65 nm diameter pores, whose features are 1 order of magnitude smaller than those previously demonstrated for sol–gel molding. We show that the high modulus of PMMA is necessary to preserve small features with high aspect ratios on the mold for nanopatterning. The molds are prepared by thermally infiltrating PMMA into anodic alumina templates, whose pore dimensions and depths are adjustable by varying anodization conditions. The difficulties associated with mold release from a master are avoided by wet etching the template. These titania films, and others made with other semiconductors, could be useful for photovoltaic, photocatalytic, and sensing applications where nanostructuring of surfaces with controlled dimensions are essential.

Nanostructured semiconductor materials have drawn a lot of attention because they exhibit interesting optical, electronic, and catalytic properties. Semiconductor films with a dense array of pores at the 10−50 nm length scale are attractive for photovoltaics,[1−4] photocatalytics,[5,6] and sensing applications.[7] For these applications, it is desirable to pattern semiconductors in a relatively simple and cheap process. Although soft lithography[8] and nanoimprint lithography[9] are promising ways to nanopattern materials, they both have limitations and may not be suitable for patterning certain materials and specifications. Soft lithography, which usually utilizes elastomer poly(dimethylsiloxane) (PDMS) molds, has been extensively used to pattern photoresists, biological macromolecules, and semiconducting polymers.[8,10] The resolution achievable with PDMS however has often been limited to >100 nm due to its relatively low compression modulus of ∼2 MPa.[11] The use of a harder version of PDMS (h-PDMS) with a compression modulus of ∼9 MPa has increased the resolution to about 50 nm,[11,12] but only for features that are not densely spaced together and of high aspect ratio. This points to the need for an even harder mold as patterning is pushed toward increasingly smaller scale. Nanoimprint lithography, which has formidable resolution approaching 5 nm,[13] uses a hard Si or SiO_2 mold to achieve high aspect ratio features. Nanoimprinted materials include photoresists, polymers, silicon, and sol−gel materials,[9,14−16] but some other materials cannot be patterned by nanoimprint lithography because the mold adheres to the film and cannot be removed. For instance, nanostructuring of sol−gel inorganics potentially useful in many low cost applications can be very challenging with either soft lithography or nanoimprint lithography. Here, we demonstrate molding of sol−gel precursors to make nanostructured metal oxide films, whose features are 1 order of magnitude smaller than those previously demonstrated for sol−gel molding.[15,17]

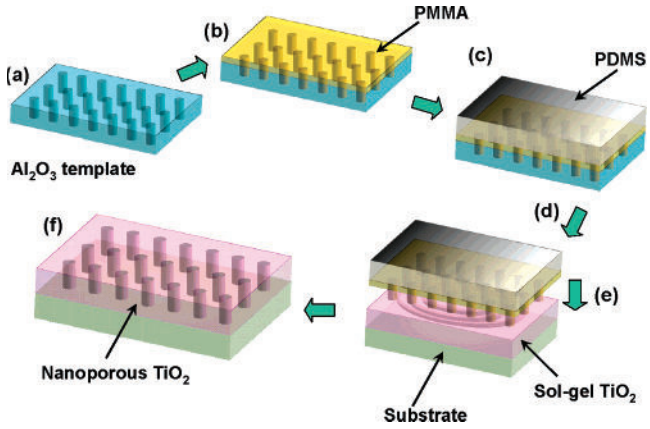

Figure 1. Schematic diagram of the processes involved in embossing titania: (a) preparing AAO template, (b) infiltrating PMMA, (c) coating on PDMS, (d) retrieving mold by wet chemical etching, (e) embossing sol−gel TiO_2, and (f) removing the mold.

We show that embossing with a hard polymer mold can be an attractive alternative to pattern nanoporous films in a relatively simple process (Figure 1). Specifically, we nanostructure titania (TiO_2) films from sol−gel precursors to resemble the structure of an anodic alumina (AAO) template with pore diameters of 35−65 nm. It was recently reported

* Corresponding author. E-mail: mmcgehee@stanford.edu.

10.1021/nl050704c CCC: $30.25
Published on Web 07/26/2005

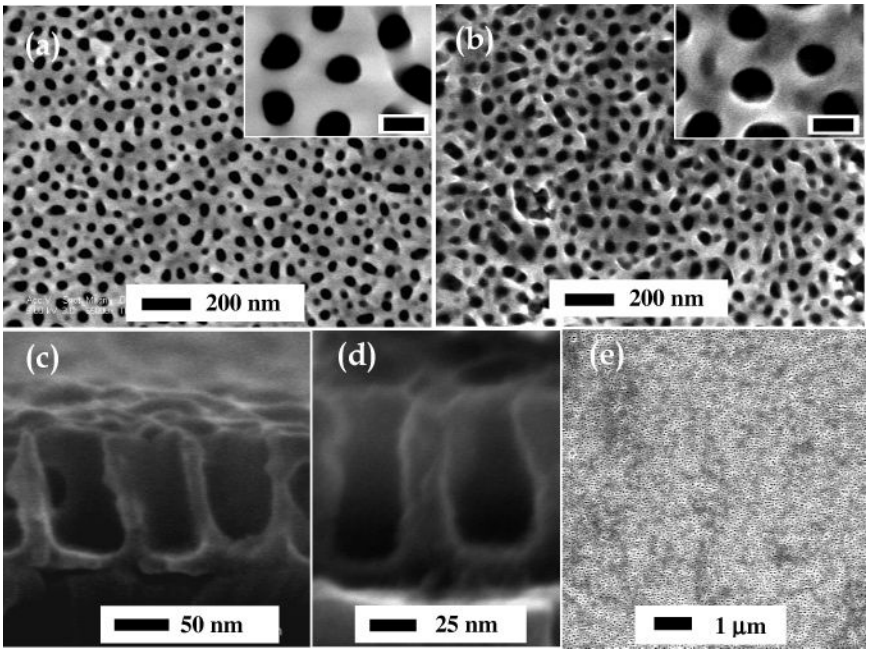

Figure 2. SEM images of (a) typical initial AAO template, (b) typical embossed TiO_2 structures after PMMA removal with acetonitrile, the average pore diameter is 45 nm, (c) embossed TiO_2 structures on FTO substrate after calcinations (cross section), the average pore diameter is larger because the initial template used has larger pore diameter, (d) smaller-diameter pores with one showing 30 nm diameter, and (e) embossed TiO_2 at a larger scale showing uniformity of the replication. The insets in (a) and (b) are respectively images at a higher magnification; the scale bar corresponds to 50 nm.

that nanoimprint lithography can be used to fabricate titania gratings with 300-nm pitch from sol−gel solution.[15] The patterned features were one-dimensional and sinusoidal in topography, which allows easier release of the mold from the condensed TiO_2. Here we report fabricating two-dimensional (2D) patterns with spacing of 100 nm and aspect ratios approaching 2 to 3. Our approach makes use of poly(methyl methacrylate) (PMMA) as the mold material. The high compression modulus (∼2−3 GPa) of PMMA allows higher-resolution patterning to be achieved, compared to PDMS, because PMMA can retain its structure without distortion before the pattern transfer into TiO_2. PMMA was also chosen due to several other properties that it possesses. Our approach draws reference from earlier works using PMMA to replicate the structure of anodic alumina master,[18,19] but we have improved on the method by preparing the TiO_2 film on useful substrates and controlling the thickness uniformity. PMMA can readily fill the template either by polymerizing the monomers[18,19] inside the template or, as is shown here, by thermally infiltrating the polymer itself. The AAO masters with desired dimensions can be easily prepared without any lithographic methods; therefore the dimensions in the final nanoporous films can be readily modified by preparing the master accordingly. The mold is retrieved by wet etching the master to avoid various mechanical issues related to mold release. The actual pattern transfer happens when the mold is embossed onto TiO_2 precursor solution (or precursors of other materials) while allowing the solution to dry with the mold in place. Once the TiO_2 condenses and solidifies, the mold can be dissolved away. Choosing to dispose of the mold instead of reusing it opens up new opportunities in terms of achievable resolution.

The starting anodic alumina template was prepared by electron-beam evaporating 500 nm of aluminum on a glass substrate and anodizing the aluminum in an anodization bath with a platinum mesh as the counter electrode (Figure 1a). The anodization conditions for making AAO are well documented in the literature;[20,21] the pore spacing and pore diameters can be tuned by using different acidic baths with certain voltages, while the depth of the pores (the thickness of the anodized aluminum layer) is controlled by adjusting the anodization time. The aluminum was anodized in a 0.3 M oxalic acid bath at 17 °C with 40 V for 120−160 s. The thickness of the alumina film obtained was between 140 and 200 nm. The alumina template was subsequently pore widened in 1 M phosphoric acid for 18 min to achieve an average pore size of 45 nm. A scanning electron microscopy (SEM) top view of a typical AAO template is shown in Figure 2a.

Molds were made by filling the anodic alumina with PMMA (Figure 1b). A thin layer (<250 nm) of PMMA with a molecular mass of 350 kg/mol was spin coated from a chlorobenzene solution onto the AAO template. The sample was subsequently heated to 200 °C, significantly above its glass transition temperature of 120 °C, to drive the polymer into the pores of the AAO.[9,22] It was found with SEM that the maximum final TiO_2 structure's height obtained with the PMMA mold does not correspond to the starting template pore depths. We attribute this to air trapped at the bottom of the pores preventing maximum filling even under prolonged infiltration.[23] A 1-mm-thick layer of PDMS (Sylgard 184) was subsequently coated over the PMMA and cured at room temperature (Figure 1c). This PDMS layer provides the backing layer for the mold so that it can be more easily

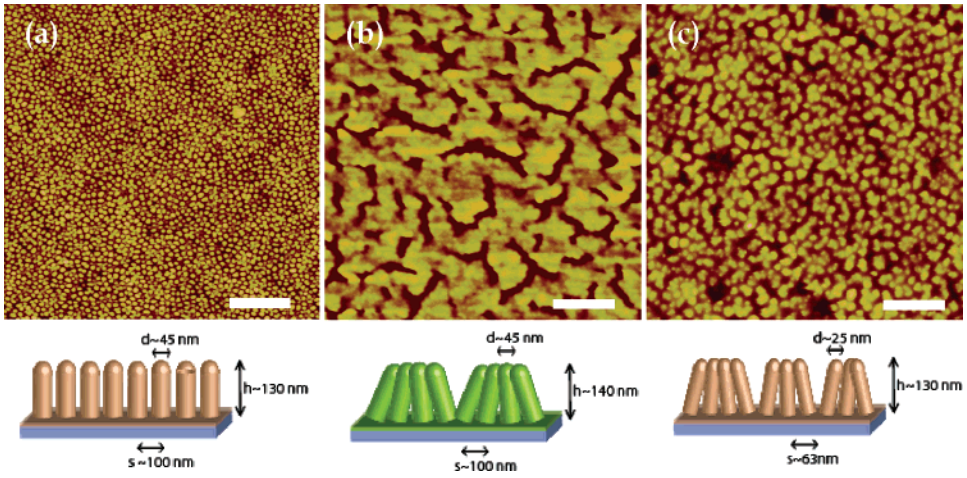

Figure 3. AFM topography images of (a) mold made from PMMA with interrod spacing (denoted s) of 100 nm, where the height (denoted h) of the rods was inferred from the final embossed TiO_2 structure, (b) mold made from h-PDMS with interrod spacing of 100 nm, where the height difference between the bright region and the dark region in the micrograph corresponds to the height of the rods, (c) mold made from PMMA with interrod spacing of 63 nm. The diameter of the rods (denoted d) in each micrograph was assumed to be that of the AAO pores. The scale bars in each image corresponds to 1 μm. The schematic below each micrograph is an illustration of what happened to the rods with the spacing, diameter, and height indicated.

manipulated, has the flexibility it needs to conform well to substrates,[11,12] and at the same time adds permeability to the solvent used for embossing. The composite mold of PMMA/PDMS was retrieved by wet etching methods (Figure 1d), first by etching in a 1.4 wt % $FeCl_3$ in 4 M HCl solution to remove the remaining aluminum beneath the AAO and then subsequently with a 10 wt % NaOH solution to remove the alumina.

The PMMA rods were free-standing in air when the appropriate spacing and aspect ratios were selected. Figure 3a shows an atomic force microscopy (AFM) image for a sample whose features had an average interrod spacing of ~100 nm, as determined by the 2D Fourier transform of the image. This average spacing is expected of an AAO template anodized in the oxalic acid solution with the condition mentioned before. The height of the PMMA rods was not resolvable by the AFM tip due to the limited gap between rods and the high aspect ratio of the structures. Its height of ~120 nm is therefore inferred from the final TiO_2 structure height. We also made a mold with h-PDMS instead of PMMA and found that the modulus contrast between the two materials resulted in very different structural integrity of the molds. h-PDMS molds were prepared according to previously published procedures.[12] Figure 3b shows the AFM image of the h-PDMS mold after being retrieved from the template. The h-PDMS rods were found to aggregate together with an average aggregation size of 500 nm. Clearly, the h-PDMS modulus is not large enough to keep the closely spaced rods from bending and sticking together by van der Waals interactions. The bending might have occurred while the mold was drying due to the surface tension of the solution pulling the rods together. A comparison of Figure 3a and Figure 3b highlights the need for the mold to be made of a hard material when patterning resolution is high. When the spacing of the rods was reduced to 63 nm and the rod diameter to 25 nm, by anodizing the template in 0.3 M sulfuric acid bath at 25 V with a subsequent pore widening time of 8 min, even the stiffer PMMA rods aggregated, as depicted in Figure 3c. This experiment suggests that if this approach is to be used for nanostructuring sol−gel inorganics at a more formidable interpore spacing of <50 nm, a mold material harder than PMMA will be necessary. The likelihood of aggregation increases as both the interrod spacing and the gap between rods becomes smaller. It is essential to point out the difference between *spacing* and *resolution* in nanopatterning; although a sub-50 nm *spacing* (distance between pore to pore) may be difficult to achieve in this case, a sub-50 nm patterning *resolution* (diameter of the pores, the thickness of the pore walls) is achievable as shown in some of the SEM images in Figure 2.

Once PMMA molds similar to the one in Figure 3a were retrieved, they were used to emboss[24,25] TiO_2 sol−gel solutions by laminating the solutions between substrates and themselves (Figure 1e). As the mold was flexible, it conformed to the substrate without any applied pressure. Embossed TiO_2 structures were prepared on various substrates including silicon wafers and indium−tin oxide coated and fluorine doped tin oxide coated (FTO) glass substrates. The sol−gel solution was prepared by mixing together 1 g of titanium(IV) ethoxide, 0.15 g of HCl and 8 g of 2-propanol. Spin coating was used to deposit the precursor solution before embossing because it allows good control of the final TiO_2 thickness uniformity. We explored two methods of embossing. The first is to spin-coat sol−gel solutions onto a substrate for a short time and emboss with the mold before the solution dried. This method however trapped air between the solution and the mold interface and resulted in a final TiO_2 structure with a high density of voids. The second method involves spin-coating the sol−gel solutions onto the mold directly and then embossing on the substrate prior to solution drying. This method draws analogy to the method of reverse nanoimprinting, whereby the nanoimprint pattern was first formed in the polymer film by directly spin coating on a nanoimprint mold before the pattern

was transferred.[16] We suspect that when the sol−gel is cast on the mold directly, the solution can permeate between the PMMA rods more readily to enable good filling, which reduces the density of voids in the TiO_2 film. After the solution dried, the PDMS was peeled off while the PMMA adhered strongly to the TiO_2. The PMMA was removed by dissolving in acetonitrile. The porous TiO_2 film was finally calcined in air to crystallize the titania and completely remove the organic residuals (Figure 1f).

An SEM image of a nanoporous TiO_2 film obtained after removal of the PMMA mold with acetonitrile (Figure 2b) shows that the initial pattern of the AAO template (Figure 2a) is preserved in the final TiO_2 structure. The significance of this replication is that the features were spaced very closely at the tens of nanometer length scale, which itself is a major challenge in nanopatterning. A cross sectional SEM in Figure 2c shows that the pores in the TiO_2 extend to a depth of ∼120 nm. This depth was confirmed by repeated casting of the sol−gel on the mold, which resulted in only an increase in the underlayer of the film with no increase in the feature heights. The fabrication of larger pore diameters of 50−70 nm in Figure 2c, obtained in this case by adjusting the template pore widening time accordingly, highlights the integrity of the pore walls that is not only thin but also tall. We note that not all pores look like those in Figure 2c, as bent (nonstraight) pores were also observed. Due to the distribution of pore sizes in the initial template which is carried over to the final structure, the TiO_2 film contains different pore sizes, as exemplified by Figure 2d. An examination of Figure 2c and Figure 2d shows the feats of this patterning approach, which includes aspect ratios of the pores of 2 to 3 and of the pore walls approaching 4 to 5, and the tunability of the pore diameters, with the smallest pore demonstrated being 30 nm in diameter. A top view at a larger scale of a film in Figure 2e demonstrates that the replication is uniform across a large area. Replication regions as large as 200 × 200 μm without any major defects could be found.

The choice of PMMA as the replicating material should be elaborated. First, it has a higher modulus compared to most organic materials, which ensures that dense and small features can be replicated in the mold without distortions. Second, PMMA is highly processible. It can be dissolved in organic solvents and spin cast into a thin film. It can also be thermally heated to assist infiltration into the AAO template. Third, it is stable in both aqueous and alcohol solutions. This allows the mold to remain intact while being exposed to caustic solutions of $FeCl_3$/HCl and NaOH, which are used for retrieving the mold from the template. The use of wet etching thus allows the complete preservation of template features at the nanoscale, without breaking, adhesion of the mold to the template, or other mechanical failures usually associated with mold release from a master.[26,27] Fourth, the stability of PMMA in alcohols ensures that it does not dissolve in 2-propanol, which is used to prepare the TiO_2 sol−gel solutions. Finally, PMMA can be dissolved away with organic solvents without disrupting the nanoporous titania.

To investigate the crystallinity of the TiO_2 films, X-ray diffraction was performed on a film that was calcined at 450 °C for 6 h. A 2θ scan shows a peak at 25.3° corresponding to the (101) peak of anatase TiO_2. This crystal structure is expected of TiO_2 films made through the sol−gel method and calcined below 600 °C.[28] As our patterning method involves several steps involving wet processes, it is important to check for surface contamination in the final TiO_2 structures that might be carried over from earlier steps. X-ray photoelectron spectroscopy (XPS) measurements on the surface of the film with 1% sensitivity for elemental detection found only background signal of carbon and no signal from metal ion contaminants from $FeCl_3$, NaOH, or Al_2O_3.

The replication of the patterns occurred throughout the area of a mold. A typical mold size was around 0.5−1 cm^2. An even larger pattern transfer area can be achieved with this method, but the process will eventually be limited by the etching of the AAO template. As the AAO template is covered with both PMMA and PDMS, the etching process occurs from the sides of the template, with etchant diffusion in the lateral direction being the limiting step. The thickness of the embossed TiO_2 can ideally be tuned to even larger thickness, for instance, if increased surface area is desired. With the TiO_2 sol−gel recipe and calcination conditions that were used, it was found that a maximum thickness of ∼150 nm could be achieved before film cracking was encountered. The cracking occurred because the condensation of the sol−gel film induced tensile stress. While the variation of the pore sizes in the final structure may appear large, it originated from the starting template. With increasing ordering in the initial AAO template, the variation of the diameters and interpore spacings in the final structures can be accordingly reduced. Ordering can be achieved by two-step anodization[29,30] or indentation of aluminum top surface to initiate pore formation.[31,32] Although we have only shown here nanostructuring of TiO_2, it is straightforward to extend this method to other metal oxides made from sol−gel solutions. This allows a versatile investigation of varied properties of the metal oxides while keeping the geometrical factor the same. This process can be also be used to emboss nanocrystals and organic materials such as conjugated polymers, provided the solution does not dissolve the mold.

In summary, we have solved several challenging problems that are often encountered when embossing materials at the nanoscale and have developed a series of techniques that can be used to create periodic structures in a variety of semiconductors. Specifically, we have used anodic alumina as a template to avoid using electron-beam lithography. We used thermal infiltration to fill the narrow pores with mold material. We used a thin layer of PMMA covered with a thick layer of PDMS as the mold so that the mold would be permeable, but mechanically stable and flexible. We etched the anodic alumina to avoid damaging the mold during retrieval from the template. Finally, we dissolved the mold after embossing the semiconductor to prevent sticking. These techniques have enabled us to pattern dense arrays of deep, narrow, straight pores in titania, a semiconductor that is often used in photovoltaic and photocatalytic applications.

Acknowledgment. This work was supported by a Kodak Research Fellowship and the Global Climate and Energy Project at Stanford University.

References

(1) O'Regan, B.; Schwartz, D. T.; Zakeeruddin, S. M.; Gratzel, M. *Adv. Mater.* **2000**, *12*, 1263−1267.
(2) Yang, F.; Shtein, M.; Forrest, S. R. *Nat. Mater.* **2005**, *4*, 37−41.
(3) Shaheen, S. E.; Ginley, D. S.; Jabbour, G. E. *MRS Bull.* **2005**, *30*, 10−19.
(4) Coakley, K. M.; McGehee, M. D. *Chem. Mater.* **2004**, *16*, 4533−4542.
(5) Rajeshwar, K.; de Tacconi, N. R.; Chenthamarakshan, C. R. *Chem. Mater.* **2001**, *13*, 2765−2782.
(6) Adachi, M.; Murata, Y.; Harada, M.; Yoshikawa, S. *Chem. Lett.* **2000**, 942−943.
(7) Varghese, O. K.; Gong, D. W.; Paulose, M.; Ong, K. G.; Dickey, E. C.; Grimes, C. A. *Adv. Mater*. **2003**, *15*, 624−627.
(8) Xia, Y. N.; Whitesides, G. M. *Angew. Chem., Int. Ed. Engl.* **1998**, *37*, 551−575.
(9) Chou, S. Y.; Krauss, P. R.; Renstrom, P. J. *Science* **1996**, *272*, 85−87.
(10) Granlund, T.; Nyberg, T.; Roman, L. S.; Svensson, M.; Inganas, O. *Adv. Mater.* **2000**, *12*, 269−273.
(11) Schmid, H.; Michel, B. *Macromolecules* **2000**, *33*, 3042−3049.
(12) Odom, T. W.; Love, J. C.; Wolfe, D. B.; Paul, K. E.; Whitesides, G. M. *Langmuir* **2002**, *18*, 5314−5320.
(13) Austin, M. D.; Ge, H. X.; Wu, W.; Li, M. T.; Yu, Z. N.; Wasserman, D.; Lyon, S. A.; Chou, S. Y. *Appl. Phys. Lett.* **2004**, *84*, 5299−5301.
(14) Chou, S. Y.; Keimel, C.; Gu, J. *Nature* **2002**, *417*, 835−837.
(15) Li, M. T.; Tan, H.; Chen, L.; Wang, J.; Chou, S. Y. *J. Vac. Sci. Technol., B*: *Microelectron Nanometer Struct.*−*Process., Meas., Phenom.* **2003**, *21*, 660−663.
(16) Guo, L. J. *J. Phys. D*: *Appl. Phys.* **2004**, *37*, R123−141.
(17) Yang, P. D.; Wirnsberger, G.; Huang, H. C.; Cordero, S. R.; McGehee, M. D.; Scott, B.; Deng, T.; Whitesides, G. M.; Chmelka, B. F.; Buratto, S. K.; Stucky, G. D. *Science* **2000**, *287*, 465−467.
(18) Masuda, H.; Nishio, K.; Baba, N. *Jpn. J. Appl. Phys.* **1992**, *31*, L1775−L1777.
(19) Masuda, H.; Fukuda, K. *Science* **1995**, *268*, 1466−1468.
(20) Li, F. Y.; Zhang, L.; Metzger, R. M. *Chem. Mater.* **1998**, *10*, 2470−2480.
(21) Li, A. P.; Muller, F.; Birner, A.; Nielsch, K.; Gosele, U. *J. Appl. Phys.* **1998**, *84*, 6023−6026.
(22) Coakley, K. M.; Liu, Y. X.; McGehee, M. D.; Frindell, K. L.; Stucky, G. D. *Adv. Funct. Mater.* **2003**, *13*, 301−306.
(23) Kim, D. H.; Lin, Z. Q.; Kim, H. C.; Jeong, U.; Russell, T. P. *Adv. Mater.* **2003**, *15*, 811−814.
(24) Cavallini, M.; Murgia, M.; Biscarini, F. *Nano Lett.* **2001**, *1*, 193−195.
(25) Ziebarth, J. M.; Saafir, A. K.; Fan, S.; McGehee, M. D. *Adv. Funct. Mater.* **2004**, *14*, 451−456.
(26) Bietsch, A.; Michel, B. *J. Appl. Phys.* **2000**, *88*, 4310−4318.
(27) Hui, C. Y.; Jagota, A.; Lin, Y. Y.; Kramer, E. J. *Langmuir* **2002**, *18*, 1394−1407.
(28) Ovenstone, J.; Yanagisawa, K. *Chem. Mater.* **1999**, *11*, 2770−2774.
(29) Masuda, H.; Satoh, M. *Jpn. J. Appl. Phys.* **1996**, *35*, L126−129.
(30) Li, A. P.; Muller, F.; Birner, A.; Nielsch, K.; Gosele, U. *Adv. Mater.* **1999**, *11*, 483−487.
(31) Masuda, H.; Yamada, H.; Satoh, M.; Asoh, H.; Nakao, M.; Tamamura, T. *Appl. Phys. Lett.* **1997**, *71*, 2770−2772.
(32) Asoh, H.; Nishio, K.; Nakao, M.; Tamamura, T.; Masuda, H. *J. Electrochem. Soc.* **2001**, *148*, B152−156.

NL050704C